

## ORIGINAL ARTICLE

# Sclerostin blockade promotes bone metastases of Wnt-responsive breast cancer cells

Toru Hiraga<sup>1</sup>  | Kanji Horibe<sup>1</sup> | Masanori Koide<sup>2</sup> | Teruhito Yamashita<sup>2</sup> | Yasuhiro Kobayashi<sup>2</sup>

<sup>1</sup>Department of Histology and Cell Biology, Matsumoto Dental University, Nagano, Japan

<sup>2</sup>Institute for Oral Science, Matsumoto Dental University, Nagano, Japan

**Correspondence**

Toru Hiraga, Department of Histology and Cell Biology, Matsumoto Dental University, 1780 Gobara-Hirooka, Shiojiri, Nagano 399-0781, Japan.  
Email: [toru.hiraga@mdu.ac.jp](mailto:toru.hiraga@mdu.ac.jp)

**Funding information**

Japan Society for the Promotion of Science, Grant/Award Number: 18K19656 and 21K09863

**Abstract**

The secreted protein sclerostin is primarily produced by osteocytes and suppresses osteoblast differentiation and function by inhibiting the canonical Wnt signaling pathway. Genetic and pharmacological inhibition of sclerostin has been shown to increase bone formation and an anti-sclerostin antibody has been clinically approved for the treatment of osteoporosis. Canonical Wnt signaling is also involved in the progression of several types of cancers including breast cancer. Here, we studied the effects of sclerostin inhibition on the development of bone metastases of breast cancer using mouse models. TOPFLASH assay and real-time PCR analysis of *AXIN2*, a target of canonical Wnt signaling, revealed that, among four cell lines tested, MDA-MB-231 human breast cancer cells responded highly to the canonical Wnt ligand Wnt3a, whereas other cell lines exhibited marginal responses. Consistent with these results, treatment with an anti-sclerostin antibody significantly increased the bone metastases of MDA-MB-231 but not those of other breast cancer cells. Immunohistochemical studies demonstrated that an anti-sclerostin antibody induced intracellular accumulation of  $\beta$ -catenin in bone-colonized MDA-MB-231 cells. Suspension culture assays showed that Wnt3a accelerated the tumorsphere formation of MDA-MB-231 cells, whereas monolayer cell proliferation and migration were not affected. Furthermore, the numbers of osteoclasts and their precursor cells in bone metastases of MDA-MB-231 were significantly increased in mice treated with an anti-sclerostin antibody. These results collectively suggest that sclerostin blockade activates canonical Wnt signaling in ligand-responsive breast cancer cells metastasized to bone, thereby increasing bone metastases, likely to have been mediated at least in part by enhancing stem cell-like properties of cancer cells and osteoclastogenesis.

**KEYWORDS**

bone metastasis, breast cancer, canonical Wnt signaling, osteoclasts, sclerostin

**Abbreviations:** DKK1, Dickkopf-1; LRP, low-density lipoprotein receptor-related protein; PGE<sub>2</sub>, prostaglandin E<sub>2</sub>; PTHrP, parathyroid hormone-related protein; TRAP, tartrate-resistant acid phosphatase.

This is an open access article under the terms of the [Creative Commons Attribution-NonCommercial-NoDerivs](https://creativecommons.org/licenses/by-nc-nd/4.0/) License, which permits use and distribution in any medium, provided the original work is properly cited, the use is non-commercial and no modifications or adaptations are made.

© 2023 The Authors. *Cancer Science* published by John Wiley & Sons Australia, Ltd on behalf of Japanese Cancer Association.

## 1 | INTRODUCTION

Sclerostin, the *Sost* gene product, is a secreted protein that acts as an inhibitor of canonical Wnt signaling by binding to the Wnt co-receptors LRP5/6.<sup>1,2</sup> Sclerostin is predominantly expressed by osteocytes and physiologically regulates bone metabolism, especially suppressing bone formation. These findings indicate that the inhibition of sclerostin leads to activating canonical Wnt signaling, resulting in an increase in bone formation. In fact, *Sost*-deficient mice exhibited a marked increase in bone volume caused by enhanced bone formation.<sup>3</sup> Neutralizing monoclonal antibodies (mAbs) against sclerostin have been proven to increase bone mass in both experimental animals and humans.<sup>4</sup> Recently, romosozumab, a humanized anti-sclerostin antibody, was clinically approved for the treatment of postmenopausal osteoporosis.<sup>2</sup>

Bone is one of the most frequent target organs for breast cancer metastasis.<sup>5</sup> Accumulating evidence suggests that the initiation and progression of bone metastases are largely regulated by the bone microenvironment.<sup>5</sup> The canonical Wnt pathway has been suggested to be involved in various aspects of the progression of several types of cancers, including metastasis.<sup>6,7</sup> Considering the fact that canonical Wnt signaling plays critical roles in bone metabolism,<sup>8</sup> cancer cells colonized in bone are most likely to be under the influence of a similar environment. These findings led us to hypothesize that sclerostin blockade promotes bone metastases by enhancing canonical Wnt signaling in cancer cells. However, to date, the effects of sclerostin on bone metastases of breast cancer are still unclear.<sup>9,10</sup>

Thus, in the present study, we examined the effects of sclerostin inhibition on bone metastases of breast cancer using animal models with an anti-sclerostin antibody and *Sost*-deficient mice. The results showed that treatment with an anti-sclerostin antibody specifically increases bone metastases of breast cancer cells that can respond to canonical Wnt ligands.

## 2 | MATERIALS AND METHODS

### 2.1 | Antibodies and reagents

The anti-sclerostin antibody romosozumab and recombinant mouse Wnt3a were purchased from Amgen and BioLegend, respectively. All other reagents used in this study were purchased from Sigma-Aldrich or FUJIFILM Wako Pure Chemical Corporation unless otherwise specified.

### 2.2 | Cell cultures

The mouse breast cancer cell line 4T1 was a generous gift from Dr. Fred R. Miller (Michigan Cancer Foundation).<sup>11</sup> E0771/Bone, a highly bone metastatic clone of the mouse breast cancer cell line E0771, was established from parental E0771 cells (CH3 Biosystems) by serial *in vivo* selection as described previously.<sup>12</sup> Human breast cancer

cell lines MDA-MB-231 and MCF-7 and the rat osteosarcoma cell line UMR-106 were purchased from the ATCC. Cells were cultured in DMEM (FUJIFILM Wako Pure Chemical Corporation) supplemented with 10% FBS (Mediatech) and 100 µg/mL kanamycin sulfate (Meiji Seika Pharma) and were maintained in a humidified atmosphere of 5% CO<sub>2</sub> in air at 37°C.

### 2.3 | T-cell factor luciferase reporter assay

T-cell factor reporter plasmid TOPFLASH (Upstate Biotechnology) and Renilla luciferase control reporter plasmid (pRL-TK, Promega) were co-transfected into tumor cells plated in 24-well plates using TransIT-LT1 transfection reagent (TaKaRa Bio) in accordance with the manufacturer's instructions. Wnt3a (50 ng/mL) was added 24 h later and the cells were cultured for an additional 24 h. Luciferase activity was measured using a Dual-Luciferase Reporter Assay System (Promega). All data were normalized to Renilla luciferase controls. Data are expressed as the fold changes compared with the controls. Each assay was conducted in quadruplicate.

### 2.4 | Cell proliferation in monolayer cultures

Cell proliferation in monolayer cultures was determined using a WST-8 assay as described previously.<sup>12,13</sup> The cells were cultured in the presence or absence of Wnt3a (50 ng/mL) for 48 and 72 h. Data are expressed as fold changes in absorbance relative to the control at 48 h. Each assay was conducted in quadruplicate.

### 2.5 | Wound healing assay

The wound healing assay was performed as described previously.<sup>13</sup> Data are expressed as the percentage of the filled wound area, which was calculated as follows: filled wound area (%) = (original wound area - remaining wound area)/original wound area × 100. Each assay was performed in triplicate.

### 2.6 | Tumorsphere formation

Tumorsphere formation was assessed as previously described.<sup>12,13</sup> After cultivation for 6 days, the number of tumorspheres with a diameter of >200 µm was counted using light microscopy. Data are expressed as the number of tumorspheres/well. Each assay was performed in triplicate.

### 2.7 | RT-PCR

RT-PCR was performed as described previously.<sup>12</sup> Primer sequences and product sizes are listed in Tables S1 and S2. The sizes

of the fragments were confirmed by reference to a 100-bp DNA ladder.

## 2.8 | Real-time RT-PCR

Real-time RT-PCR was performed as described previously.<sup>12,13</sup> Primer sequences were as follows: mouse *Axin2*, ATGTCCTGTCTGCCAGCGTTC/CAAGCACTAGCCAGTGGGTCAG; mouse *β-actin*, CTAAGGCCAACCGTGAAAAG/ACCAGAGGCATACAGGGACA; human *AXIN2*, GATATCCAGTGATGCGCTGA/ACTGCCACACGATAAGGAG; human *DKK1*, CAGGCGTGCAAATCTGTCT/AATGATTTTGATCAGAAGACACACATA; human *β-actin*, CCAACCGCGAGAAGATGA/CCAGAGGCGTACAGGGATAG, rat *Sost*, GGAAGTAGACAACAACCAGACCA/GCTGTACTCGGACACGTCTTT, rat *β-actin*, CCCGCGAGTACAACCTTCT/CGTCATCCATGGCGAACT. Melting curve analysis was performed to determine the melting temperatures of the amplified products and exclude undesired primer dimers. Quantification was normalized using *β-actin* as a reference gene. Expression levels of the specific genes are indicated as fold changes compared with the controls.

## 2.9 | Animal experiments

BALB/c (female, 6-week-old), C57BL/6 (female, 8-week-old), and athymic nude (female, 6-week-old) mice were purchased from Japan SLC. *Sost-Green* reporter mice were generated, in which the 184-bp *Sost* coding sequence in exon 1 was replaced with ZsGreen coding sequence.<sup>14</sup> Homozygous *Sost<sup>Green/Green</sup>* mice on a C57BL/6 background were used as *Sost*-deficient mice. 4T1 and MDA-MB-231 cells were inoculated into BALB/c and athymic nude mice, respectively. E0771/Bone cells were inoculated into wild-type (WT) C57BL/6 or *Sost*-deficient mice. All animal experiments were approved by the Animal Management Committee of Matsumoto Dental University. The number of mice used in each experiment is described in the figure legends.

### 2.9.1 | Effects of anti-sclerostin antibody on bone volume in nontumor-bearing mice

Mice received subcutaneous injections of anti-sclerostin antibody (25 mg/kg) twice a week for 4 weeks.<sup>15</sup>

### 2.9.2 | Effects of anti-sclerostin antibody on mammary tumor formation

Mice received an intramammary injection of tumor cells (1 million cells/0.1 mL PBS/mouse).<sup>12,13</sup> The administration of anti-sclerostin antibody (25 mg/kg, s.c., twice a week) was started 1 week before

tumor inoculation, and mice were sacrificed 4 weeks after cell inoculation. Tumor volume was estimated using the following equation: Tumor volume (mm<sup>3</sup>) = (length) × (width)<sup>2</sup> × 0.5.

### 2.9.3 | Effects of anti-sclerostin antibody on bone metastases

Tumor cells (0.2 million cells/0.1 mL PBS/mouse) were inoculated through the caudal artery as described previously.<sup>16</sup> Treatment with the anti-sclerostin antibody (25 mg/kg, s.c., twice a week) was started 1 week before tumor inoculation. Mice inoculated with 4T1 and E0771/Bone were sacrificed 2 weeks after the cell inoculation. Mice inoculated with MDA-MB-231 were sacrificed at 3 weeks.

### 2.9.4 | Bone metastases and mammary tumor formation in *Sost*-deficient mice

For the bone metastases experiment, *Sost*-deficient mice were inoculated with E0771/Bone cells (0.2 million cells/0.1 mL PBS/mouse) through the caudal artery and were sacrificed at 2 weeks. For the mammary tumor formation experiment, *Sost*-deficient mice received an intramammary injection of E0771/Bone cells (1 million cells/0.1 mL PBS/mouse) and were sacrificed at 4 weeks.

## 2.10 | Histological and histomorphometric analysis

Paraffin sections were prepared using conventional methods and were stained with H&E.

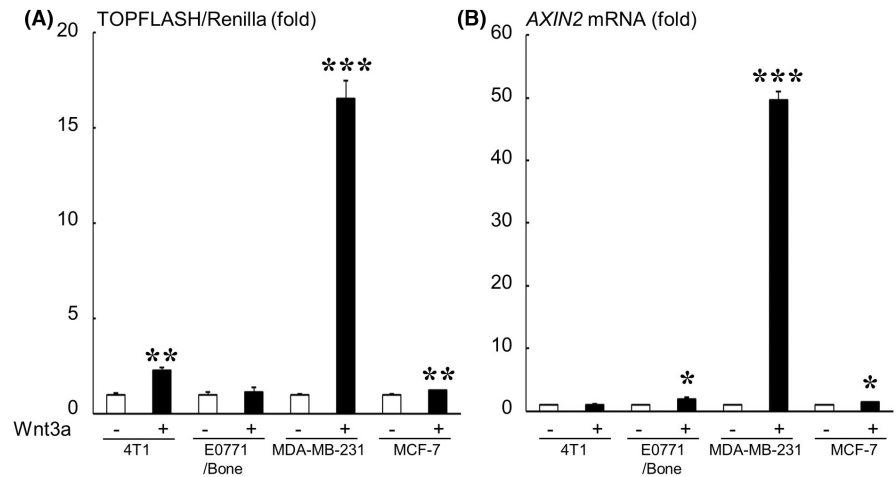
### 2.10.1 | Enzyme histochemistry

Tartrate-resistant acid phosphatase, a marker enzyme for osteoclasts, was detected as described previously.<sup>12</sup> The slides were counterstained with hematoxylin. Data were expressed as the number of TRAP-positive osteoclasts/mm bone surface or the number of TRAP-positive cells/mm<sup>2</sup> tumor area.

### 2.10.2 | Immunohistochemistry

Dewaxed paraffin sections were quenched with 0.3% hydrogen peroxide in methanol and blocked with 3% bovine serum albumin in PBS. For anti-sclerostin immunohistochemistry, antigen retrieval was performed using proteinase K (20 μg/mL) for 15 min at room temperature.<sup>17</sup> The sections were incubated with goat anti-sclerostin antibody (AF1589, R&D Systems) or rabbit anti-β-catenin antibody (sc-7199, Santa Cruz Biotechnology) overnight at 4°C, and then treated with a Histofine Simple Stain Kit (Nichirei Biosciences)

**FIGURE 1** Responsiveness of breast cancer cells to Wnt3a determined using a TOPFLASH assay (A) and real-time PCR analysis of *AXIN2* (B). Data are expressed as fold changes compared with the Wnt3a (-) control in each cell line. \*\*\* $p < 0.001$ , \*\* $p < 0.01$ , \* $p < 0.05$  compared with each control.



for 60 min at room temperature. Chromogen was developed using DAB Liquid System (Dako). The slides were counterstained with hematoxylin.

### 2.10.3 | Histomorphometry

Histomorphometric analysis of tumor burden in bone was conducted as described previously.<sup>12,13</sup> Data are expressed as the tumor area (mm<sup>2</sup>).

### 2.11 | Micro-computed tomography ( $\mu$ CT) analysis

The undecalcified femurs were subjected to  $\mu$ CT analysis using microfocus X-ray computed tomography (ScanXmate-A080; Comscantecno). The reconstruction of three-dimensional digital images and the calculation of trabecular bone volume/tissue volume (BV/TV) were conducted using TRI/3DBON software (Ratoc System Engineering).

### 2.12 | ELISA

Bone marrow fluid was collected from femurs and tibiae with 1 mL PBS.<sup>14</sup> Concentrations of sclerostin in plasma and bone marrow fluid were determined using ELISA kits (R&D systems) in accordance with the manufacturer's instructions.

### 2.13 | Statistical analysis

Data are expressed as the mean  $\pm$  SEM. Significance was analyzed using Student's *t*-test or Welch's *t*-test (Mini StatMate; ATMS). One-way ANOVA followed by Tukey's test was used when more than two groups were compared. *p*-values  $< 0.05$  were considered to be significant.

## 3 | RESULTS

### 3.1 | Responsiveness of breast cancer cells to canonical Wnt stimulation

We first examined the responsiveness of breast cancer cells to a canonical Wnt ligand Wnt3a using a TOPFLASH assay and real-time PCR analysis of *AXIN2*, a target gene of canonical Wnt signaling.<sup>18</sup> Wnt3a markedly increased TOPFLASH activity and *AXIN2* mRNA expression in MDA-MB-231 cells but only marginally affected those in other cells (Figure 1). The mRNA expression of Wnt ligands, receptors, and inhibitors in the breast cancer cells was determined using conventional RT-PCR analysis (Figure 2).

### 3.2 | Effects of sclerostin inhibition on the development of mammary tumors and bone metastases

*In vivo* experiments were conducted using 4T1, E0771/Bone, and MDA-MB-231 cells because the tumorigenicity and bone metastatic potential are not high enough in MCF-7 cells.<sup>19,20</sup>

To determine the effects of sclerostin inhibition on the development of mammary tumors and bone metastases *in vivo*, we first used a pharmacological approach. Treatment with an anti-sclerostin antibody showed no significant effect on the growth of all tumors studied in the mammary fat pads (Figure 3A–C). The development of bone metastases of 4T1 and E0771/Bone was also not affected by the antibody (Figure 4A,B). In contrast, bone metastases formation of MDA-MB-231 was significantly accelerated in mice receiving anti-sclerostin antibody (Figure 4C). We then conducted similar experiments by inoculating E0771/Bone cells of C57BL/6 origin into syngeneic *Sost*-deficient mice. Consistent with the results obtained using the anti-sclerostin antibody, the development of both mammary tumors and bone metastases of E0771/Bone was not different between WT and *Sost*-deficient mice (Figures 3D and 4D).

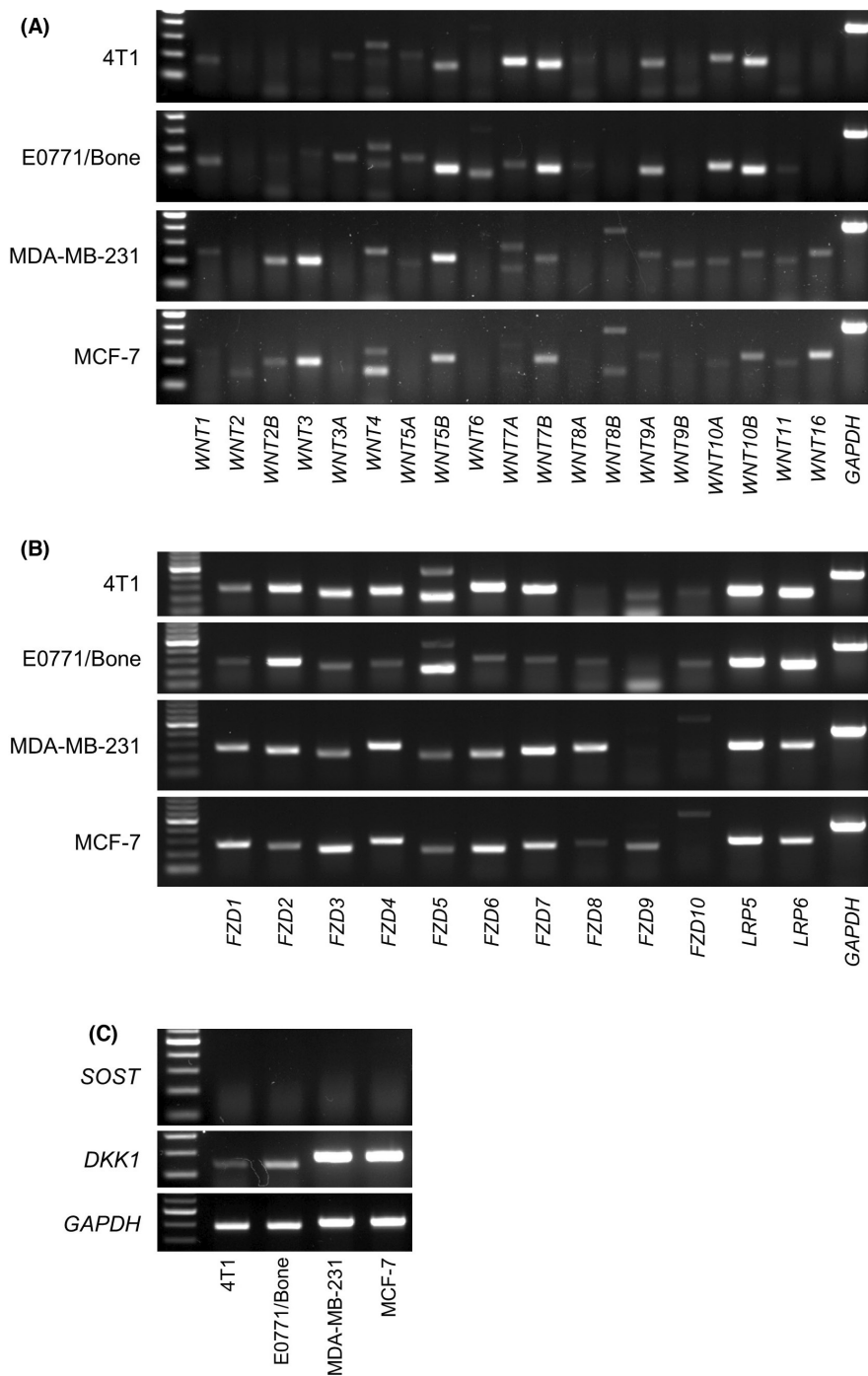


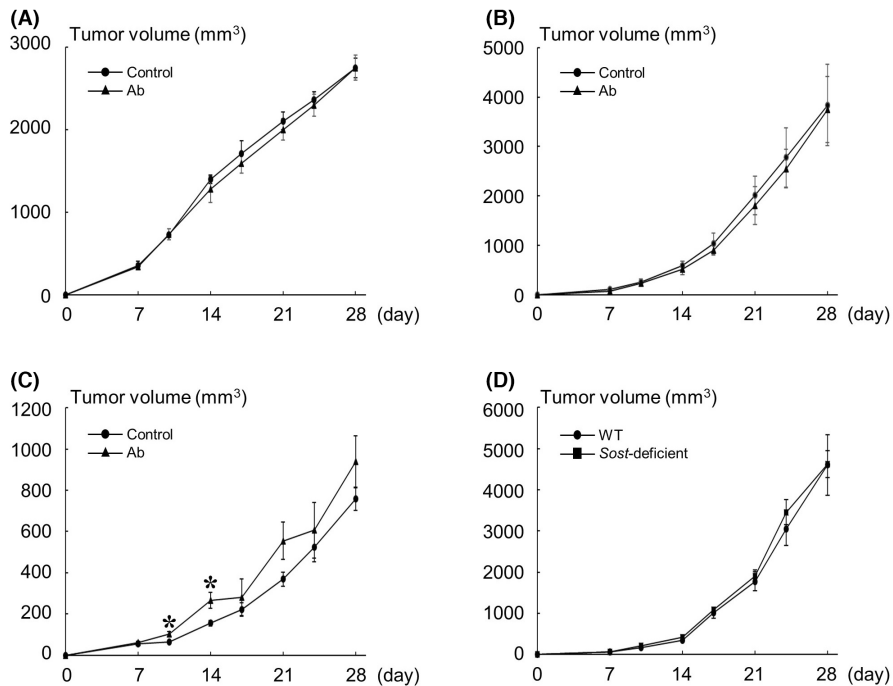
**FIGURE 2** RT-PCR analysis of mRNA expression of Wnt ligands (A), receptors (B), and inhibitors (C) in breast cancer cells (30 cycles for all analyses except for 25 cycles for GAPDH).

To confirm whether sclerostin inhibition activated canonical Wnt signaling in bone-colonized cancer cells, the expression of  $\beta$ -catenin was examined by immunohistochemistry. In the canonical Wnt pathway, Wnt ligands cause the cytoplasmic accumulation of  $\beta$ -catenin, which translocates to the nucleus to induce the expression of target genes.<sup>8</sup> Although no evident nuclear localization was seen, cytoplasmic accumulation of  $\beta$ -catenin was found in MDA-MB-231 cells in mice treated with the anti-sclerostin antibody but not in 4T1 and E0771/Bone cells (Figure 4E).

### 3.3 | Effects of Wnt3a on cell proliferation, wound healing, and tumorsphere formation *in vitro*

To explain the mechanisms by which canonical Wnt signals enhanced the development of bone metastases of MDA-MB-231 cells, the effects of Wnt3a on cell proliferation, migration, and tumorsphere formation were evaluated *in vitro*. Wnt3a exhibited no effects on monolayer cell proliferation and migration of MDA-MB-231 cells determined using a WST-8 assay and wound healing assay (Figure S1);

**FIGURE 3** Effects of sclerostin inhibition on tumor growth in the orthotopic mammary fat pads. (A–C) Effects of the anti-sclerostin antibody (Ab) on the growth of 4T1 (A,  $n = 5$ ), E0771/Bone (B,  $n = 6$ ), and MDA-MB-231 (C,  $n = 8$ ) tumors in the mammary fat pads. (D) Tumor growth of E0771/Bone in the mammary fat pads in *Sost*-deficient mice ( $n = 8$ ). Data are expressed as tumor volume ( $\text{mm}^3$ ). \* $p < 0.05$ .



however, tumorsphere formation was significantly increased by Wnt3a (Figure 5A).

We also found that the anti-sclerostin antibody treatment increased the number of TRAP-positive osteoclasts and their precursor cells on bone surfaces and in tumor nests in bone metastases of MDA-MB-231 (Figure 5B). Real-time PCR analysis showed that Wnt3a increased the expression of *DKK1*, a target of canonical Wnt signaling,<sup>18</sup> in MDA-MB-231 cells (Figure 5C).

### 3.4 | Effects of tumor burden on the expression of sclerostin in mice

We finally studied the local and systemic effects of tumor burden on sclerostin expression in mice. The concentration of mouse sclerostin in plasma measured using ELISA was not changed in mice bearing mammary tumors and bone metastases (Figure 6A). Conversely, mammary tumor burden significantly reduced the sclerostin concentration in bone marrow fluid, but bone metastases exerted no effects (Figure 6A).

To examine if these changes were caused by tumor cells, UMR-106 rat osteosarcoma cells, which constitutively express *Sost*,<sup>14</sup> were cultured with tumor conditioned medium. Real-time PCR analysis showed that the conditioned medium markedly downregulated *Sost* mRNA expression (Figure 6B). The effects were equivalent to or more potent than the positive control PTHrP.<sup>21</sup> Conventional RT-PCR analysis showed that all tested cancer cells expressed *PTHrP* mRNA (Figure 6C). Immunohistochemical analysis demonstrated that the expression of sclerostin in osteocytes in cortical bone was markedly decreased in areas adjacent to cancer cells colonized in bone compared with those adjacent to neighboring normal bone marrow (Figure 6D).

## 4 | DISCUSSION

The main action of sclerostin is thought to be the inhibition of canonical Wnt signaling.<sup>1</sup> If this is true, the principal mechanism of action of anti-sclerostin treatment is the reactivation of the canonical Wnt pathway. To date, several papers have reported the effects of genetic or pharmacologic blockade of sclerostin on bone metastases of breast cancer and multiple myeloma in mice.<sup>9,10,22,23</sup> Considering that bone formation was increased by sclerostin inhibition, canonical Wnt signaling was activated in the bone microenvironment in these models. However, whether the signal was transduced into tumor cells remained undetermined. Therefore, we examined the responsiveness of breast cancer cells to the canonical Wnt ligand Wnt3a and found it greatly variable among the cell lines (Figure 1). MDA-MB-231 cells were highly responsive to Wnt3a stimulation but the others were not. Furthermore, the anti-sclerostin antibody induced intracellular accumulation of  $\beta$ -catenin in MDA-MB-231 cells (Figure 4E), suggesting that antibody treatment activated the canonical Wnt signaling in MDA-MB-231 cells metastasized to bone. These results agreed with the finding that the treatment with anti-sclerostin antibody increased only the bone metastases of MDA-MB-231 (Figure 4A–C). Of note, a previous similar study done by Hesse et al. reported that an anti-sclerostin antibody decreased the bone metastatic tumor burden of MDA-MB-231.<sup>10</sup> The reasons for this discrepancy are unclear, although the experimental protocols are somewhat different between the two studies. One definite difference is the antibodies used: we used a humanized mAb romosozumab, whereas Hesse et al. used a fully human mAb setrusumab (BPS804).<sup>24</sup> Another important difference is the treatment schedules. We started the treatment 1 week before tumor cell inoculation, whereas Hesse et al. started treatment 2 weeks after inoculation. Our protocol might work efficiently to facilitate the initial development

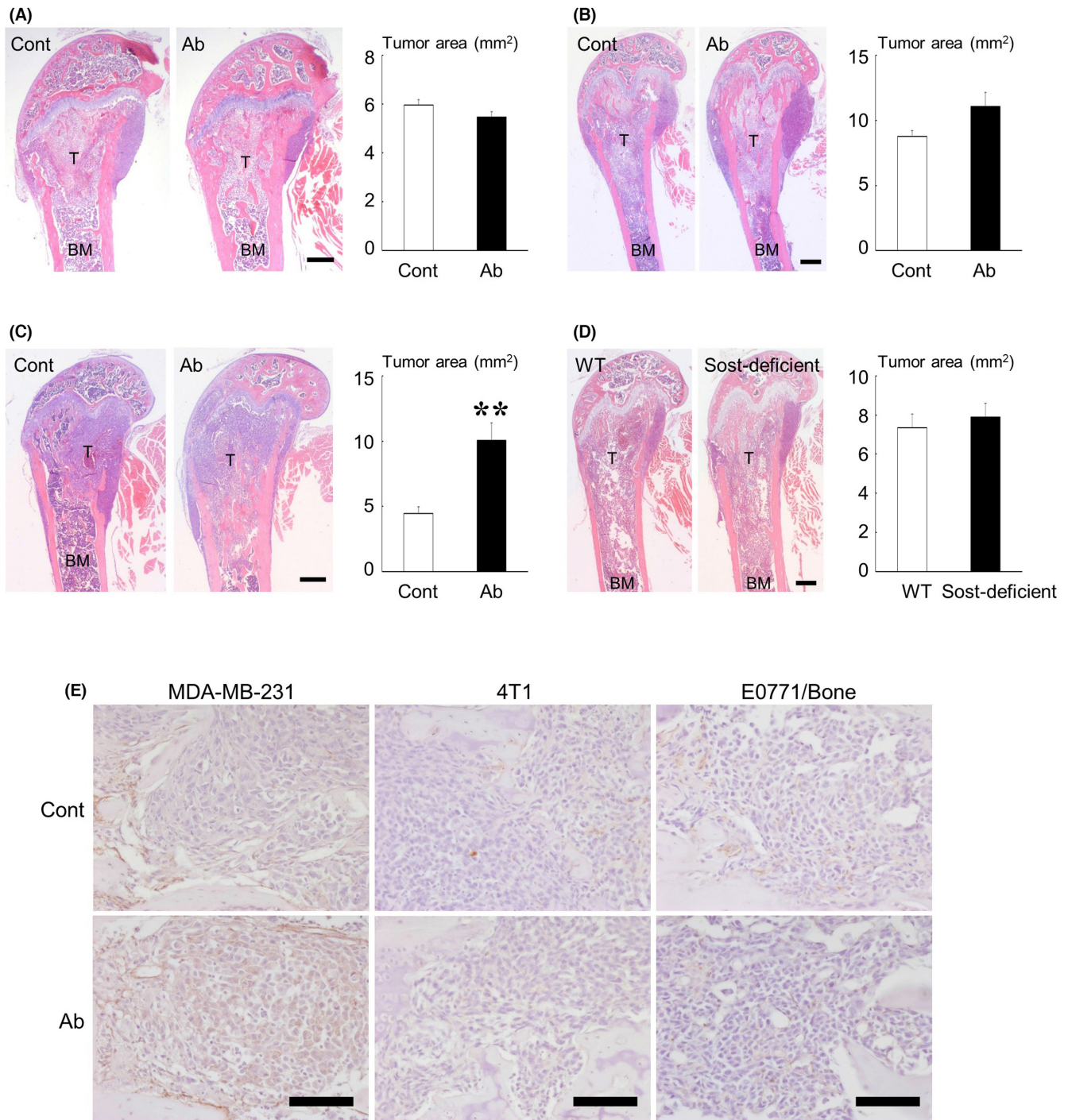


**FIGURE 4** Effects of sclerostin inhibition on the development of bone metastases. (A–C) Effects of the anti-sclerostin antibody (Ab) on bone metastases of 4T1 (A,  $n = 9$ ), E0771/Bone (B,  $n = 8$ ), and MDA-MB-231 (C,  $n = 6$ ). (D) Bone metastases of E0771/Bone in *Sost*-deficient mice ( $n = 10$ ). Representative histologic views of bone metastases are shown on the left (H&E staining; T, tumor; BM, bone marrow; scale bars = 500 μm). Data are expressed as tumor area (mm<sup>2</sup>). \*\* $p < 0.01$ . (E) Immunohistochemical study of β-catenin in bone metastases of MDA-MB-231, 4T1, and E0771/Bone treated without or with anti-sclerostin antibody (scale bars = 100 μm).

of bone metastases of MDA-MB-231 by preparing a canonical Wnt ligand-rich premetastatic bone microenvironment. In contrast with bone metastases, the anti-sclerostin antibody given using a similar protocol did not affect the progression of mammary tumors, which is likely to have been due to low systemic levels of sclerostin compared with bone marrow (Figure 6A). Our data implicated that the use of

an anti-sclerostin antibody in osteoporotic patients with a history of breast cancer should be considered with caution.

To understand the reason for the variation in responsiveness to the canonical Wnt ligand Wnt3a among the cell lines, the expression of Wnt ligands, receptors, and inhibitors was examined (Figure 2). Even though the expression patterns and levels were different, all

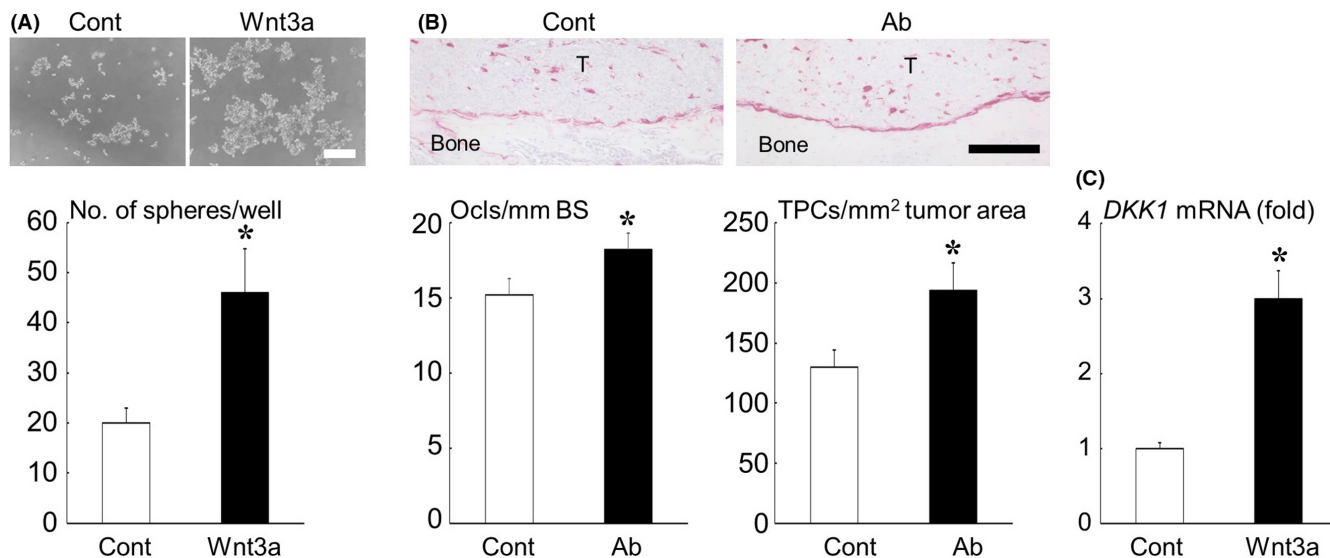
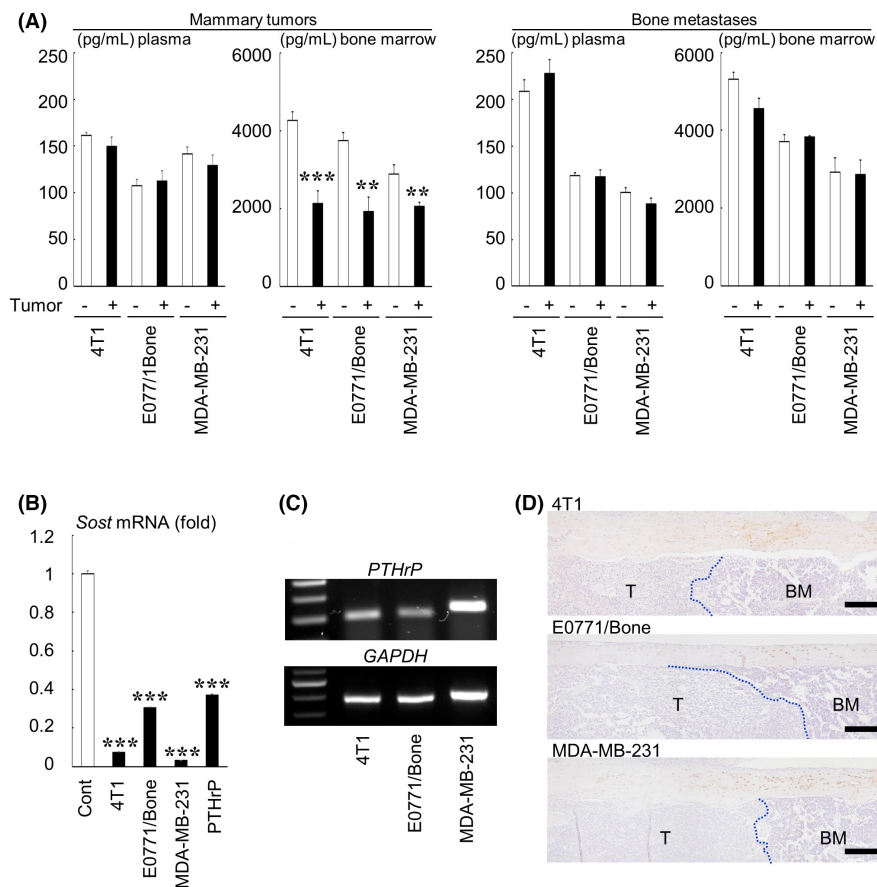


**FIGURE 5** (A) Effects of Wnt3a on tumorsphere formation of MDA-MB-231 cells in suspension culture. Representative microscopic images are shown at the top (scale bar = 500  $\mu$ m). Data are expressed as the number of tumorspheres/well. (B) Effects of the anti-sclerostin antibody (Ab) on the number of TRAP-positive osteoclasts at the tumor-bone interface and TRAP-positive osteoclast precursor cells in tumor nests in bone metastases of MDA-MB-231. Representative histologic views are shown at the top (TRAP staining; T, tumor; scale bar = 200  $\mu$ m). Data are expressed as the number of TRAP-positive osteoclasts/mm bone surface (Ocls/mm BS) or the number of TRAP-positive cells/mm<sup>2</sup> tumor area (TPCs/mm<sup>2</sup> tumor area). (C) Effects of Wnt3a on mRNA expression of *DKK1* in MDA-MB-231 cells determined by real-time RT-PCR analysis. Data are expressed as fold changes compared with the control. \* $p < 0.05$ .

**FIGURE 6** Effects of tumor burden on the sclerostin production and expression in mice. (A) The concentration of sclerostin in plasma and bone marrow fluid in mice bearing mammary tumors and bone metastases as determined using ELISA ( $n = 4$ ). \*\*\* $p < 0.001$ , \*\* $p < 0.01$  compared with each control. (B) Relative mRNA expression of *Sost* in UMR-106 cells treated with conditioned medium from breast cancer cells or PTHrP (1  $\mu$ g/mL) determined by real-time RT-PCR. Data are expressed as fold changes compared with the control. \*\*\* $p < 0.001$  compared with the control. (C) RT-PCR analysis of mRNA expression of *PTHrP* in breast cancer cells (30 cycles for *PTHrP*, 25 cycles for *GAPDH*). (D) Immunohistochemical analysis of the sclerostin expression in bone metastases of breast cancer. The dotted lines indicate the border between metastatic tumor nests (T) and adjacent normal bone marrow (BM) (scale bars = 200  $\mu$ m).



cell lines expressed several kinds of Wnt receptors. It is currently unknown which molecules determine the responsiveness to Wnt3a. Any other downstream signaling molecules of the canonical Wnt

pathway may also play a key role. Since none of the tumor cells expressed *SOST* mRNA (Figure 2C), it is unlikely that sclerostin acted in an autocrine manner in these tumor cells. Further studies are



needed to predict the responsiveness of breast cancer cells to canonical Wnt ligands.

Consistent with previous reports,<sup>25</sup> Wnt3a significantly enhanced the tumorsphere formation of MDA-MB-231 cells in suspension culture (Figure 5A). Tumorsphere-forming ability is widely accepted as a property of cancer stem-like cells.<sup>26</sup> Our previous studies suggested that cancer stem-like cells have higher bone metastatic potential.<sup>13,27</sup> Thus, sclerostin blockade probably increased bone metastases of MDA-MB-231, at least in part, by enhancing cancer stem-like properties through the activation of canonical Wnt signaling.

The histological study showed that the number of TRAP-positive osteoclasts and their precursor cells was increased in bone metastases of MDA-MB-231 in mice treated with anti-sclerostin antibody (Figure 5B). Because osteoclastic bone destruction plays critical roles in the development and progression of bone metastases,<sup>5</sup> the promotion of osteoclastogenesis is another possible mechanism for enhanced bone metastasis formation by sclerostin inhibition. Our data also showed that Wnt3a increased the mRNA expression of *DKK1* in MDA-MB-231 cells (Figure 5C). *DKK1* has been shown to decrease the expression and production of osteoprotegerin,<sup>28,29</sup> a potent inhibitor of osteoclast differentiation,<sup>30</sup> in osteoblastic cells, which may account for the increased number of osteoclastic cells caused by treatment with the anti-sclerostin antibody. A report by Johnson et al.<sup>31</sup> that Wnt3a increased the expression of PTHrP, a potent stimulator of osteolysis, in MDA-MB-231 cells also supports our results.

Some molecules, such as PTH, PTHrP, and PGE<sub>2</sub> are known to downregulate sclerostin expression.<sup>1</sup> *PTHrP* was expressed in 4T1, E0771/Bone, and MDA-MB-231 cells (Figure 6C). 4T1 and MDA-MB-231 cells were also shown to produce PGE<sub>2</sub>.<sup>32,33</sup> Consistent with these findings, conditioned medium from these cancer cells markedly decreased sclerostin expression in UMR-106 cells (Figure 6B). Furthermore, the sclerostin concentration in bone marrow was significantly reduced in mice bearing mammary tumors (Figure 6A). These results suggest that the soluble factors, including PTHrP and PGE<sub>2</sub>, derived from the tumors decreased sclerostin production in bone (Figure 6A). Immunohistochemical analysis also revealed that the osteocytes adjacent to metastatic cancer cells lost sclerostin expression (Figure 6D). Nevertheless, the sclerostin concentrations in plasma and bone marrow in mice with bone metastases remained unchanged (Figure 6A). The tumor burden in bone, which was much smaller than mammary tumors and mostly localized only in the distal part of the femurs and the proximal part of the tibias, might not be high enough to significantly change the sclerostin levels in plasma and whole bone marrow. Feedback mechanisms also might work to maintain the sclerostin levels.

One issue of the current study we are aware of is that the anti-sclerostin antibody romosozumab used in this study is a humanized mAb. The use of this antibody in mice may develop an anti-human antibody response, thereby causing inactivation and elimination of the antibody from the blood, resulting in loss of therapeutic efficacy or adverse effects.<sup>4</sup> Romosozumab was shown to have the ability to neutralize mouse sclerostin as well as human sclerostin

*in vitro*.<sup>34</sup> Several studies have so far used romosozumab in rodent studies and showed that romosozumab increased bone volume.<sup>35–37</sup>

Furthermore, our preliminary study demonstrated that romosozumab markedly increased bone volume in all species of mice used in this study (Figure S2). No obvious adverse reactions were observed in any mice receiving romosozumab in our study. It is thus likely that romosozumab exerts its own biological effects in mice at least in relatively short-term experiments.

A limitation of this study is that MDA-MB-231 cells could not be tested in *Sost*-deficient mice. This was because human-derived MDA-MB-231 cells are not tumorigenic in *Sost*-deficient mice with an immunocompetent C57BL/6 background. Because immunodeficient nude mice were used for experiments with MDA-MB-231 cells, the immunocompromised host microenvironment may also need to be taken into consideration when interpreting the effects of sclerostin blockade. In this context, several studies have suggested that the activation of canonical Wnt signaling is associated with an immunosuppressive microenvironment in various types of cancer.<sup>38,39</sup>

In conclusion, our results collectively suggested that sclerostin blockade enhances canonical Wnt signaling in ligand-responsive breast cancer cells colonized in bone, thereby increasing bone metastases, probably mediated, at least in part, by promoting stem cell-like properties of cancer cells and osteoclastogenesis. Caution may be necessary when anti-sclerostin therapy is given to osteoporotic patients with a history of breast cancer. A screening method needs to be developed to predict the responsiveness of breast cancer cells to canonical Wnt ligands.

#### AUTHOR CONTRIBUTIONS

Toru Hiraga: Conceptualization, Methodology, Validation, Formal analysis, Investigation, Writing – original draft, review & editing, Visualization, Supervision, Project administration, Funding acquisition. Kanji Horibe: Investigation. Masanori Koide: Writing – review & editing. Teruhito Yamashita: Resources, Writing – review & editing. Yasuhiro Kobayashi: Resources, Writing – review & editing.

#### FUNDING INFORMATION

This work was supported by grants from JSPS KAKENHI (Grant numbers 18K19656 and 21K09863), Japan.

#### ACKNOWLEDGEMENT

None.

#### CONFLICT OF INTEREST STATEMENT

The authors declare no conflict of interest.

#### ETHICAL APPROVAL

Approval of the research protocol by an Institutional Reviewer Board: N/A.

Informed consent: N/A.

Registry and the Registration No. of the study/trial: N/A.

Animal studies: All animal experiments were approved by the Animal Management Committee of Matsumoto Dental University.

## ORCID

Toru Hiraga  <https://orcid.org/0000-0002-7829-2395>

## REFERENCES

- Iwamoto R, Koide M, Udagawa N, Kobayashi Y. Positive and negative regulators of sclerostin expression. *Int J Mol Sci.* 2022;23:4895. doi:10.3390/ijms23094895
- Tanaka S, Matsumoto T. Sclerostin: from bench to bedside. *J Bone Miner Metab.* 2021;39:332-340. doi:10.1007/S00774-020-01176-0
- Li X, Ominsky MS, Niu QT, et al. Targeted deletion of the sclerostin gene in mice results in increased bone formation and bone strength. *J Bone Miner Res.* 2008;23:860-869. doi:10.1359/JBMR.080216
- Ominsky MS, Boyce RW, Li X, Ke HZ. Effects of sclerostin antibodies in animal models of osteoporosis. *Bone.* 2017;96:63-75. doi:10.1016/j.bone.2016.10.019
- Hiraga T. Bone metastasis: interaction between cancer cells and bone microenvironment. *J Oral Biosci.* 2019;61:95-98. doi:10.1016/j.job.2019.02.002
- Parsons MJ, Tammela T, Dow LE. WNT as a driver and dependency in cancer. *Cancer Discov.* 2021;11:2413-2429. doi:10.1158/2159-8290.CD-21-0190
- Zhan T, Rindtorff N, Boutros M. Wnt signaling in cancer. *Oncogene.* 2017;36:1461-1473. doi:10.1038/ONC.2016.304
- Maeda K, Kobayashi Y, Koide M, et al. The regulation of bone metabolism and disorders by Wnt signaling. *Int J Mol Sci.* 2019;20:5525. doi:10.3390/ijms20225525
- Zhu M, Liu C, Li S, Zhang S, Yao Q, Song Q. Sclerostin induced tumor growth, bone metastasis and osteolysis in breast cancer. *Sci Rep.* 2017;7:1-10. doi:10.1038/s41598-017-11913-7
- Hesse E, Schröder S, Brandt D, Pamperin J, Saito H, Taipaleenmäki H. Sclerostin inhibition alleviates breast cancer-induced bone metastases and muscle weakness. *JCI Insight.* 2019;5:e125543. doi:10.1172/jci.insight.125543
- Aslakson CJ, Miller FR. Selective events in the metastatic process defined by analysis of the sequential dissemination of subpopulations of a mouse mammary tumor. *Cancer Res.* 1992;52:1399-1405.
- Hiraga T, Ninomiya T. Establishment and characterization of a C57BL/6 mouse model of bone metastasis of breast cancer. *J Bone Miner Metab.* 2019;37:235-242. doi:10.1007/s00774-018-0927-y
- Hiraga T, Ito S, Nakamura H. EpCAM expression in breast cancer cells is associated with enhanced bone metastasis formation. *Int J Cancer.* 2016;138:1698-1708. doi:10.1002/ijc.29921
- Koide M, Yamashita T, Murakami K, et al. Sclerostin expression in trabecular bone is downregulated by osteoclasts. *Sci Rep.* 2020;10:13751. doi:10.1038/s41598-020-70817-1
- Li X, Ominsky MS, Warmington KS, et al. Sclerostin antibody treatment increases bone formation, bone mass, and bone strength in a rat model of postmenopausal osteoporosis. *J Bone Miner Res.* 2009;24:578-588. doi:10.1359/JBMR.081206
- Kuchimaru T, Kataoka N, Nakagawa K, et al. A reliable murine model of bone metastasis by injecting cancer cells through caudal arteries. *Nat Commun.* 2018;9:2981. doi:10.1038/s41467-018-05366-3
- Sato T, Verma S, Andrade CDC, et al. A FAK/HDAC5 signaling axis controls osteocyte mechanotransduction. *Nat Commun.* 2020;11:3282. doi:10.1038/s41467-020-17099-3
- Doumpas N, Lampart F, Robinson MD, et al. TCF/LEF dependent and independent transcriptional regulation of Wnt/ $\beta$ -catenin target genes. *EMBO J.* 2019;38:e98873. doi:10.15252/embj.201798873
- Levenson AS, Jordan VC. MCF-7: the first hormone-responsive breast cancer cell line. *Cancer Res.* 1997;57:3071-3078.
- Yi B, Williams PJ, Niewolna M, Wang Y, Yoneda T. Tumor-derived platelet-derived growth factor-BB plays a critical role in osteosclerotic bone metastasis in an animal model of human breast cancer. *Cancer Res.* 2002;62:917-923.
- de Castro LF, Lozano D, Portal-Núñez S, et al. Comparison of the skeletal effects induced by daily administration of PTHrP (1-36) and PTHrP (107-139) to ovariectomized mice. *J Cell Physiol.* 2012;227:1752-1760. doi:10.1002/JCP.22902
- Delgado-Calle J, Anderson J, Cregor MD, et al. Genetic deletion of Sost or pharmacological inhibition of sclerostin prevent multiple myeloma-induced bone disease without affecting tumor growth. *Leukemia.* 2017;31:2686-2694. doi:10.1038/leu.2017.152
- McDonald MM, Reagan MR, Youlten SE, et al. Inhibiting the osteocyte-specific protein sclerostin increases bone mass and fracture resistance in multiple myeloma. *Blood.* 2017;129:3452-3464. doi:10.1182/blood-2017-03-773341
- Glorieux FH, Devogelaer JP, Durigova M, et al. BPS804 anti-sclerostin antibody in adults with moderate osteogenesis imperfecta: results of a randomized phase 2a trial. *J Bone Miner Res.* 2017;32:1496-1504. doi:10.1002/jbmr.3143
- Lamb R, Ablett MP, Spence K, Landberg G, Sims AH, Clarke RB. Wnt pathway activity in breast cancer sub-types and stem-like cells. *PLoS One.* 2013;8:e67811. doi:10.1371/journal.pone.0067811
- Charafe-Jauffret E, Ginestier C, Iovino F, et al. Breast cancer cell lines contain functional cancer stem cells with metastatic capacity and a distinct molecular signature. *Cancer Res.* 2009;69:1302-1313. doi:10.1158/0008-5472.CAN-08-2741
- Hiraga T, Ito S, Nakamura H. Cancer stem-like cell marker CD44 promotes bone metastases by enhancing tumorigenicity, cell motility, and hyaluronan production. *Cancer Res.* 2013;73:4112-4122. doi:10.1158/0008-5472.CAN-12-3801
- Zhuang X, Zhang H, Li X, et al. Differential effects on lung and bone metastasis of breast cancer by Wnt signalling inhibitor DKK1. *Nat Cell Biol.* 2017;19:1274-1285. doi:10.1038/NCB3613
- Bu G, Lu W, Liu CC, et al. Breast cancer-derived Dickkopf1 inhibits osteoblast differentiation and osteoprotegerin expression: implication for breast cancer osteolytic bone metastases. *Int J Cancer.* 2008;123:1034-1042. doi:10.1002/IJC.23625
- Simonet WS, Lacey DL, Dunstan CR, et al. Osteoprotegerin: a novel secreted protein involved in the regulation of bone density. *Cell.* 1997;89:309-319. doi:10.1016/S0092-8674(00)80209-3
- Johnson RW, Merkel AR, Page JM, Ruppender NS, Guelcher SA, Sterling JA. Wnt signaling induces gene expression of factors associated with bone destruction in lung and breast cancer. *Clin Exp Metastasis.* 2014;31:945-959. doi:10.1007/S10585-014-9682-1
- Singh T, Katiyar SK, Honokiol A. Phytochemical from Magnolia spp., inhibits breast cancer cell migration by targeting nitric oxide and cyclooxygenase-2. *Int J Oncol.* 2011;38:769-776. doi:10.3892/IJO.2011.899
- Hiraga T, Myoui A, Choi ME, Yoshikawa H, Yoneda T. Stimulation of cyclooxygenase-2 expression by bone-derived transforming growth factor-beta enhances bone metastases in breast cancer. *Cancer Res.* 2006;66:2067-2073. doi:10.1158/0008-5472.CAN-05-2012
- Hamaya E. Pharmacological characteristics and clinical study results of romosozumab (EVENITY®; genetical recombination), a drug with novel mechanism of action to treat osteoporosis at high risk of fracture. *Folia Pharmacol Jpn.* 2020;155:258-267. doi:10.1254/fpj.20007
- Costa S, Fairfield H, Reagan MR. Inverse correlation between trabecular bone volume and bone marrow adipose tissue in rats treated with osteoanabolic agents. *Bone.* 2019;123:211-223. doi:10.1016/J.BONE.2019.03.038

36. Takase R, Tsubouchi Y, Otsu T, Kataoka T, Iwasaki T, Kataoka M. The effects of romosozumab combined with active vitamin D3 on fracture healing in ovariectomized rats. *J Orthop Surg Res.* 2022;17:384. doi:[10.1186/s13018-022-03276-1](https://doi.org/10.1186/s13018-022-03276-1)
37. Brent MB, Br uel A, Thomsen JS. Anti-sclerostin antibodies and abaloparatide have additive effects when used as a countermeasure against disuse osteopenia in female rats. *Bone.* 2022;160:116417. doi:[10.1016/j.bone.2022.116417](https://doi.org/10.1016/j.bone.2022.116417)
38. Gattinoni L, Zhong XS, Palmer DC, et al. Wnt signaling arrests effector T cell differentiation and generates CD8+ memory stem cells. *Nat Med.* 2009;15:808-813. doi:[10.1038/nm.1982](https://doi.org/10.1038/nm.1982)
39. Takeuchi Y, Tanegashima T, Sato E, et al. Highly immunogenic cancer cells require activation of the WNT pathway for immunological escape. *Sci Immunol.* 2021;6:eabc6424. doi:[10.1126/sciimmunol.abc6424](https://doi.org/10.1126/sciimmunol.abc6424)

## SUPPORTING INFORMATION

Additional supporting information can be found online in the Supporting Information section at the end of this article.

**How to cite this article:** Hiraga T, Horibe K, Koide M, Yamashita T, Kobayashi Y. Sclerostin blockade promotes bone metastases of Wnt-responsive breast cancer cells. *Cancer Sci.* 2023;114:2460-2470. doi:[10.1111/cas.15765](https://doi.org/10.1111/cas.15765)